

# JOINT PP-PS INVERSION WITH REGISTRATION OPTIMISATION TO IMPROVE GEOLOGICAL KNOWLEDGE OF A DEEP-WATER FIELD WEST AFRICA

D. Lopez<sup>1</sup>, A. Barnola<sup>2</sup>, P. Roy<sup>1</sup>, B. Roure<sup>1</sup>, J. Brunellière<sup>2</sup>

<sup>1</sup> CGG; <sup>2</sup> Total

## Summary

---

Inversion has become the standard procedure to quantify elastic properties using seismic. PP seismic is commonly used for this purpose, but in areas where PP seismic is affected by gas pockets or mud volcanoes, the reflectivity can be compromised for reservoir characterization. PP-PS inversion can step in to improve the determination of elastic properties when PP seismic inversion alone is challenging. However, the biggest challenge of this multi-component inversion lies in the registration between PP and PS information.

This abstract illustrates the application of PP-PS elastic inversion using an improved technique that includes an innovative correction of travel time to rectify for residual time registration. This case study from a deep-water field in West Africa was carried out on acquired ocean-bottom nodes (OBN) dataset. The seismic preconditioning, PP inversion, registration approach and the implementation of the advanced PP-PS inversion helped in the better characterisation of elastic properties of the reservoir.

## **Joint PP-PS Inversion with registration optimisation to improve geological knowledge of a deep-water field West Africa**

### **Introduction**

The use of PP-PS inversion has increased in offshore areas over the last few years due to the growth in OBN acquired surveys. PS seismic can help to better predict lithology properties as it is less affected by fluid effects. However, PS seismic has a much lower high frequency content and is more susceptible to noise contamination when compared to PP seismic.

The field is located offshore from West Africa and the reservoir is formed essentially by stacked turbiditic channels affected by compressional tectonics that led to intensive faulting and compartmentalisation. The area is affected by gas leakages and shallow gas pockets that made necessary the use of OBN technology to improve the imaging at the reservoir compared to conventional streamer methods.

A high quality seismic image was attained from the PP OBN processing. The benefit of imaging the PS component was assessed over a pilot area through a simultaneous PP-PS elastic inversion. The PP-PS inversion workflow showed that the registration of PS seismic in PP time domain was challenging because PP and PS images are difficult to reconcile. Indeed P and S waves do not have the same sensitivity to fluids, to lithologies and the acquired PP and PS signal characteristics differ. To tackle this problem, the inversion algorithm was adapted to cope with the remaining discrepancies left after the conventional registration workflow.

### **Method**

The non-linear inversion method applied in this study inverts angle stacks using a simulated annealing optimization technique (Coulon et al., 2006). This model-based inversion can invert for any seismic component PP, PS and SS (Roure et al., 2015; Roure and Russell, 2019) and is defined in a stratigraphic grid with layers consistent with the seismic dips. The stratigraphic grid allows to introduce an independent time axis for each seismic component and also permits inverting registered seismic in a common component axis. A three-term cost function is minimised through the perturbation of the P-velocity, S-velocity, density and the axial component,  $T$ . The first term of the cost function accounts for the amplitude misfit simultaneously for the PP and PS data. The other terms of the cost function refer to the prior model and the continuity constraints. The travel time difference between PP and PS data is handled by defining two time axes in the stratigraphic grid,  $T_{PP}$  and  $T_{PS}$ . If the registration between PP and PS data is perfect, the two time axes are equal. However, in practice, registration error can be handled by allowing the perturbation of the PS time axis as another inversion parameter, minimizing the PS misfit. The benefit of including the PS reflectivity for AVO inversion are discussed in Gray (2003).

### **Post Stack PP and PS seismic conditioning**

A comprehensive seismic analysis check showed that PP and PS amplitudes suffered from event misalignment and amplitude energy loss in areas affected by gas leakages beneath the target interval.

A time misalignment correction workflow was applied by a cross-correlation method, implementing a stretch/squeeze factor constraint that affects the interpolated shifts and protects from extreme local stretch or squeeze of the data.

Special attention was paid to the localised areas with dimmed amplitudes, which could affect the seismic stationarity for inversion. Hence, seismic amplitudes were balanced on each of the angle stacks through a 3D scaling multiplier. As shown on Figure 1, it consisted in multiplying the 3D scaling factor to the seismic data in order to rectify the amplitude dimming. The process was carried out on the full frequency spectrum of each angle stack of each seismic component (PP and PS) and consisted in the following steps:

- Computation of 3D RMS volume to capture the 3D shape and extension of the affected area.
- Use of a cut-off on RMS volume to separate the area to be balanced.
- Selection of a “good reservoir area” to be used as a reference for AVA amplitude reference.
- Splitting of the reservoir area per macro-intervals based on reservoir and vertical variation of affected area.
- 3D Scaling factor computation per macro-interval. The scaling factor is a function of 3D RMS so that the final amplitude energy appears continuous and the corrected AVA is consistent with the AVA in the “good reservoir area”.
- Smoothing of the 3D scaling factor to avoid edge effects.
- 3D Scaling factor application and final AVA quality control.

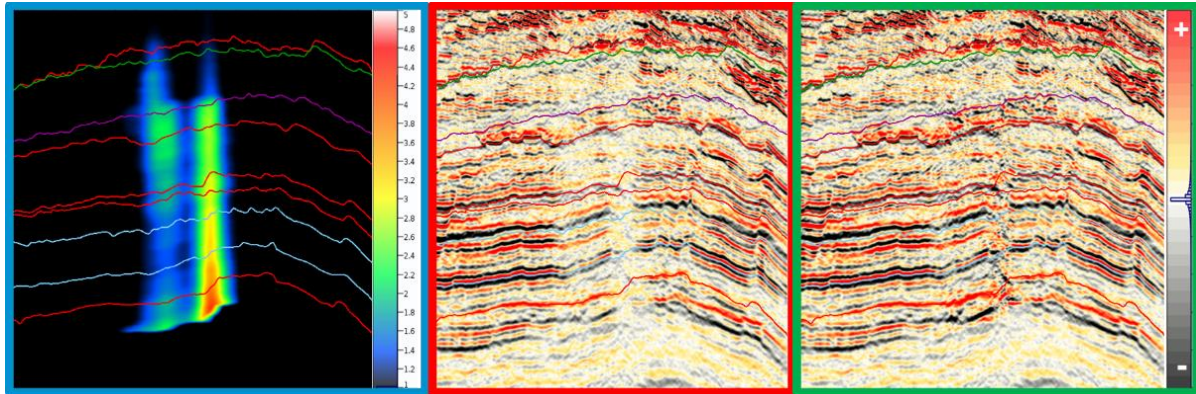


**Figure 1:** Left; 3D scaling factor. Centre; PP stack1 before amplitude balancing. Right; PP stack1 multiplied by the 3D scaling factor resulting in the amplitude balanced PP stack 1.

### PS registration

The processed PS radial component was registered to PP time, but this volume still required further improvement for PP-PS inversion. Some effort was put on improving the registration implementing a cross-correlation method. The process started by splitting the reference and registered PS seismic into 3 frequency bands; low, mid and full band. Then, time shifts are computed for the low band where a correlation coefficient threshold is used to filter out low correlated points that are later filled with a 3D spline interpolator. Later, time shifts are applied and the process starts over with the time shifts computation for the mid band and the full frequency band.

Two references for registration were assessed, (1) PS synthetics derived from PP inversion. For this, the pre-stack PP inversion was carried out to get elastic properties and PS synthetics through forward modelling. (2) The PP seismic stack 2 was flipped and filtered using a band-pass filter consistent with the PS seismic wavelet. Better registration results were attained when the PP seismic was used as the reference for registration. The reason is that the inverted S-impedance was not always perfectly honouring the S-impedance log and thus, the PS synthetics derived from logs and inversion results occasionally differed in TWT position. Despite of this, the registration proved that to get the best results, very strong reflector deformation would be required. Consequently, it was preferred to get a consistent PS image rather than a perfect registration (Figure 2).

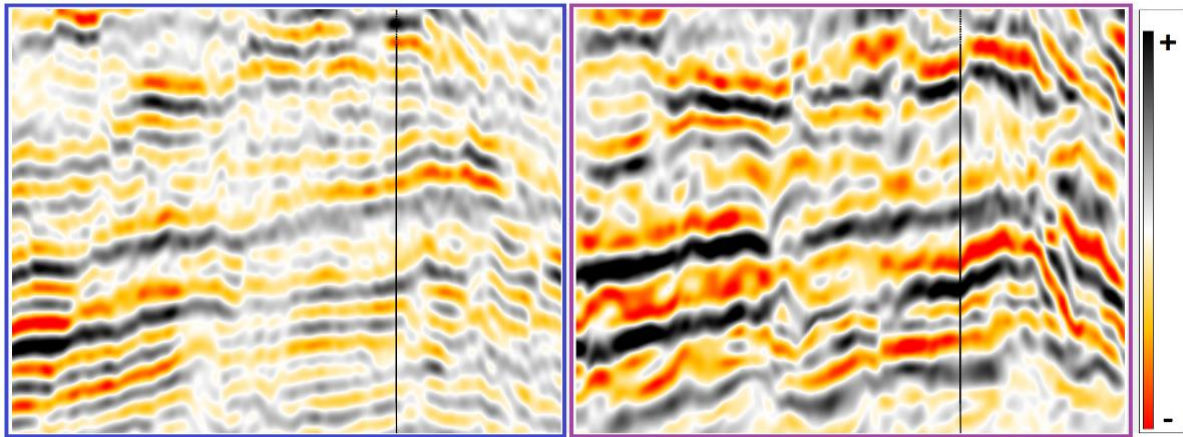


**Figure 2:** Left; PP seismic after band pass filter and polarity flipping used for PS registration. Right; Registered PS seismic. Note the large differences between left and right which makes challenging the registration step.

### PP and PP-PS elastic inversion

The PP inversion was carried out before PP-PS inversion both in two intervals to account for differences in the PP wavelet at shallow and deep intervals. Deterministic wavelets were extracted and some instabilities in the phase led to set the phase constant. The low frequency model was built implementing the PP migration velocity field and the compaction trend. Five PP angle stacks defined from  $0^\circ$  to  $42^\circ$  and four PS angle stacks between  $5^\circ$  and  $44^\circ$  were inverted. They use constraints to account for wavelet scaling optimisation, how far the inversion could move away from the initial model, lateral continuity and confidence of PP and PS stacks.

PP-PS inversion was run in two fashions: first with the  $T_{PP}$  axis only (assuming a perfect registration) and with both  $T_{PP}$  and  $T_{PS}$  axes allowing the perturbation of  $T_{PS}$  to solve any residual mismatch in the registration. Results showed that the second option managed to solve what was not attained with the registration workflow. It allowed a better match between the logs and the PP-PS inversion. This can be observed on Figures 3 and 4.

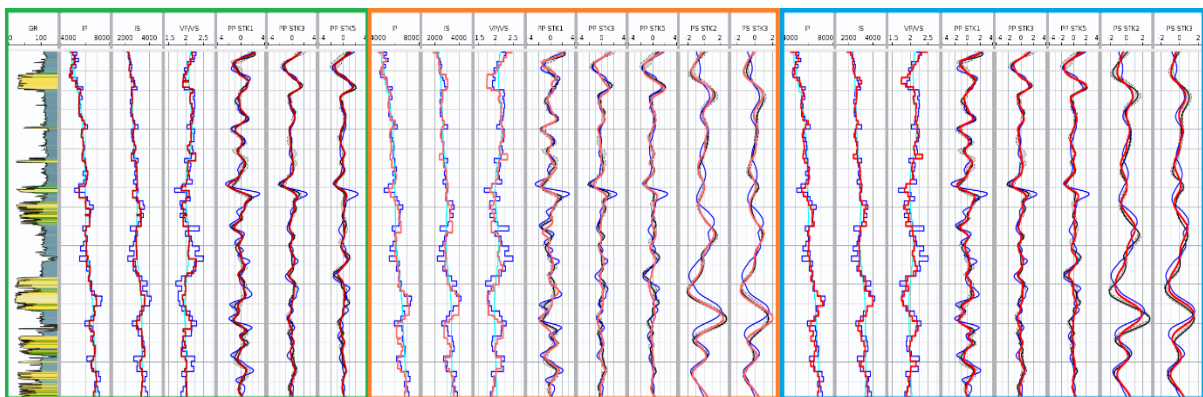


**Figure 3:** PP and PP-PS elastic inversion results for  $I_p$ ,  $I_s$  and  $V_p/V_s$ . In blue are the logs scaled at the stratigraphic grid resolution and the corresponding PP and PS synthetics. In light blue the low frequency model. In red (different tonalities) the inversion results and corresponding PP and PS synthetics. Left; PP inversion. Centre; PP-PS inversion along the optimized  $T_{PS}$  axis. Note the good match of PS seismic and synthetics but the mismatch against log derived PS-Synthetics illustrating registration issues. Right; PP-PS inversion along  $T_{PP}$  axis. A good match is achieved with logs and also the inverted synthetics are more consistent with the PS logs synthetics, accounting for the correction in the registration carried out by the inversion algorithm.

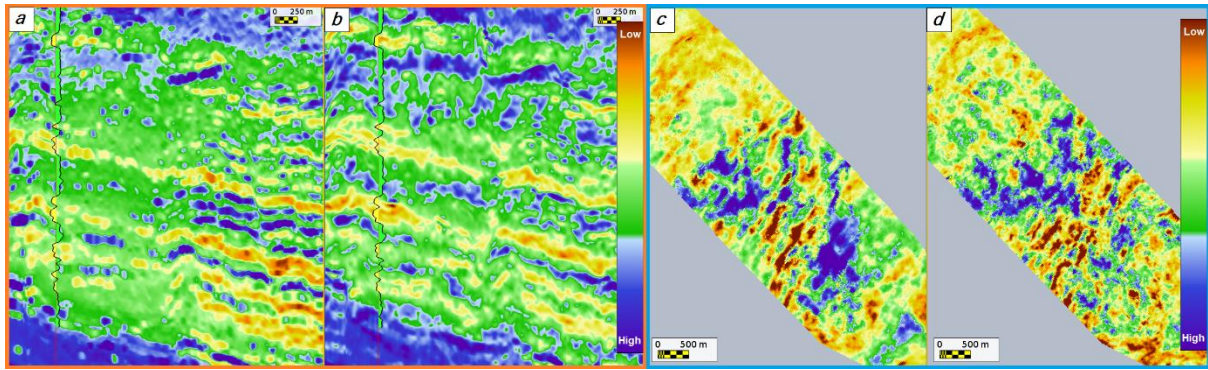


**Figure 4:** A section of  $V_p/V_s$  ratio from PP (a) and PP-PS inversion (b) are shown on the Left side of the figure crossing a vertical well which depicts the GR log. PP inversion shows good results. However, the results from the PP-PS inversion exhibit a better match and also some interesting geological features not observed in the PP inversion. On the Right are displayed maps of a  $V_p/V_s$  ratio layer from PP (c) and PP-PS inversion (d). The comparison shows that the PP-PS inverted  $V_p/V_s$  might better support fault panel and channel feature delineation when compared to the PP inversion.

## Conclusions

The PP-PS inversion with adapted registration has been successfully applied on an offshore field in West Africa. The applied workflow has demonstrated to solve challenges in the PS registration to PP component, which is deemed the more relevant and risky process for PP-PS inversion. The applied PP-PS inversion has proved to be a better approach to honour the S-impedance and thus, a more consistent  $V_p/V_s$  ratio has been attained to the well logs when compared to the PP inversion. Also, extra information was observed from the PP-PS inversion that could help in the understanding and better characterisation of the reservoir.

## Acknowledgments

We would like to thank Total HQ and affiliate and CGG for permission to present this work.

## References

- Coulon, J.-P., Lafet, Y., Deschizeaux, B., Doyen, P. M. and Duboz, P. [2006] Stratigraphic elastic inversion for seismic lithology discrimination in a turbiditic reservoir. *SEG Expanded Abstracts*, 2092-2096.
- Gray, F.D. [2003] P-S Converted-Wave AVO. *SEG Expanded Abstracts*, 165-168.
- Roure, B., Souvannavong, V., Coulon, J.-P. and Hampson, D. [2015] Joint PP-PS inversion without prior data registration. 77<sup>th</sup> EAGE Conference and Exhibition, Extended Abstract, Tu N116 04.
- Roure, B., Russell B. [2019] A preliminary look at joint PP-PS-SS inversion in native time domain. *SEG Expanded Abstracts*, 5370-5374